International Journal of Pharmaceutics 524 (2017) 397–406

Contents lists available at ScienceDirect

International Journal of Pharmaceutics

journal homepage: www.elsevier.com/locate/ijpharm

# Probing the dynamics of complexed local anesthetics via neutron scattering spectroscopy and DFT calculations

Murillo L. Martins[a,*], Juergen Eckert[b,c], Henrik Jacobsen[a,d], Éverton C. dos Santos[a,e], Rosanna Ignazzi[a], Daniele Ribeiro de Araujo[f], Marie-Claire Bellissent-Funel[g], Francesca Natali[h,i], Michael Marek Koza[i], Aleksander Matic[j], Eneida de Paula[k], Heloisa N. Bordallo[a,l]

[a] Niels Bohr Institute, University of Copenhagen, Universitetsparken 5 DK-2100, Copenhagen, Denmark
[b] Department of Chemistry, University of South Florida, 4202 E. Fowler Ave., Tampa, FL 33620, United States
[c] Theoretical Division, Los Alamos National Laboratory, Los Alamos, NM 87545, United States
[d] Department of Physics, Oxford University, Oxford, OX1 3PU, United Kingdom
[e] Department of Physics, Norwegian University of Science and Technology (NTNU), Høgskoleringen 5 NO-7491, Trondheim, Norway
[f] Human and Natural Sciences Center Federal University of ABC (UFABC) 09210–170, Santo André, SP, Brazil
[g] LLB, CEA, CNRS, Université Paris-Saclay, CEA Saclay, 91191-Gif-sur-Yvette, France
[h] Institute of Materials, Research National Council (CNR-IOM), Italy
[i] Institut Laue-Langevin, 71 Avenue des Martyrs, CS 20156, Grenoble Cedex 9, France
[j] Department of Applied Physics, Chalmers University of Technology, SE-41296 Göteborg, Sweden
[k] Department of Biochemistry and Tissue Biology, State University of Campinas (UNICAMP) 13083-862, Campinas, SP, Brazil
[l] European Spallation Source ESS P.O. Box 176, SE-22100, Lund, Sweden

ARTICLE INFO

*Article history:*
Received 3 October 2016
Received in revised form 22 March 2017
Accepted 23 March 2017
Available online 31 March 2017

*Keywords:*
Local anesthetics
Bupivacaine
Ropivacaine
HP-β-cyclodextrin
Complexation
Inelastic neutron scattering

ABSTRACT

Since potential changes in the dynamics and mobility of drugs upon complexation for delivery may affect their ultimate efficacy, we have investigated the dynamics of two local anesthetic molecules, bupivacaine (BVC, $C_{18}H_{28}N_2O$) and ropivacaine (RVC, $C_{17}H_{26}N_2O$), in both their crystalline forms and complexed with water-soluble oligosaccharide 2-hydroxypropyl-β-cyclodextrin (HP-β-CD). The study was carried out by neutron scattering spectroscopy, along with thermal analysis, and density functional theory computation. Mean square displacements suggest that RVC may be less flexible in crystalline form than BVC, but both molecules exhibit very similar dynamics when confined in HP-β-CD. The use of vibrational analysis by density functional theory (DFT) made possible the identification of molecular modes that are most affected in both molecules by insertion into HP-β-CD, namely those of the piperidine rings and methyl groups. Nonetheless, the somewhat greater structure in the vibrational spectrum at room temperature of complexed RVC than that of BVC, suggests that the effects of complexation are more severe for the latter. This unique approach to the molecular level study of encapsulated drugs should lead to deeper understanding of their mobility and the respective release dynamics.



## 1. Introduction

Local anesthetics (LAs) are amphiphile molecules widely used to attenuate or eliminate pain during medical and dental procedures. LAs in clinical use are typically amide or ester derivatives (Do Prado et al., 2006; Harmatz, 2009), formed by an aromatic ring plus an intermediate polar linker to an amine end group. Variations in the composition of these molecular groups modify the lipid/water distribution coefficient as well as the protein binding characteristics, and, consequently, alter the anesthetic potency and toxicity (McLure and Rubin, 2005). Two common LAs are Bupivacaine (BVC, $C_{18}H_{28}N_2O$) and Ropivacaine (RVC, $C_{17}H_{26}N_2O$), which are formed from one aromatic and one piperidine ring along with three methyl groups each, defined as 1, 2 and 3 as depicted in Fig. 1. The methyl group 3 in BVC, however, is

*Abbreviations:* LA, local anesthetic; BVC, bupivacaine; RVC, ropivacaine; HP-β-CD, 2-hydroxypropyl-β–cyclodextrin; DSC, differential scanning calorimetry; IINS, incoherent inelastic neutron scattering; EFW, elastic fixed-window; $E_a$, activation energy; QENS, quasielastic neutron scattering.

* Corresponding author.
*E-mail address:* murillolongo@gmail.com (M.L. Martins).

http://dx.doi.org/10.1016/j.ijpharm.2017.03.051
0378-5173/

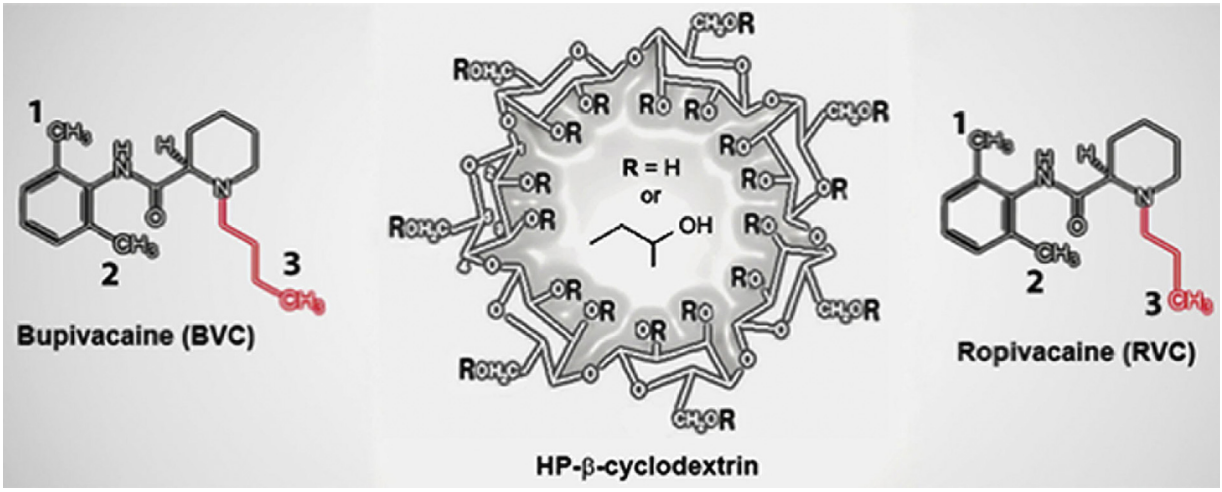


**Fig. 1.** Bupivacaine (BVC, $C_{18}H_{28}N_2O$), Ropivacaine (RVC, $C_{17}H_{26}N_2O$) and HP-β-cyclodextrin (HP-β-CD). The methyl groups of both anaesthetics are here defined as groups 1, 2 and 3 and the red colour highlights the difference between BVC and RVC side chains. For clarity, the schemes shown in the figure do not consider the molecules' packing. (For interpretation of the references to colour in this figure legend, the reader is referred to the web version of this article.)

linked by a longer side chain (butyl), with an additional carbon atom (highlighted in red in Fig. 1), relative to that in RVC (propyl). Moreover, BVC is prepared as a racemic mixture of the levo and dextro forms of the drug, while RVC corresponds to a single levorotary (S-) isomer (De Araujo et al., 2008; McLure and Rubin, 2005), which is longer acting and less toxic than the dextro form (Magalhães et al., 2004).

Due to neural and cardiac toxic effects (Albright, 1979) of BVC, which has been commercially available since 1963 (Ruetsch et al., 2001), RVC was developed and came into clinical practice in the United States in the early 1990s (Scott et al., 1989). The margin of safety for the application of RVC has, however, also become a source of controversy (Huet et al., 2003). A current approach for the reduction of toxicity has been the controlled release of LAs by their micro/nano-encapsulation or complexation into water-soluble matrixes. Along these line oligosaccharides cyclodextrins (CD) are regarded as excellent complexing agents (host) because of their pre-organized macrocyclic structure (Fig. 1), with lipophilic interior and hydrophilic exterior. HP-β-CD in particular contains 7 glucose units and is one of the most commonly used host agents because of the favorable dimensions of its cavities and its stability to complex formation with a wide range of small to medium sized guest molecules (Junco et al., 2002; Marques, 2010; Partanen et al., 2002; Rajabi et al., 2008). This compound is a derivative of β-CD, with improved water-solubility and considerable lower toxicity (Gould and Scott, 2005). The use of HP-β-CD has also been approved by the U.S. Food and Drug Administration (FDA) for infiltrative routes, and it is, for the above reasons, a highly suitable matrix for the complexation of BVC and RVC (Loftsson and Duchêne, 2007).

We must, however, assume that the complexation process results in a unique inclusion compound, with different physical properties relative to those of the free molecules. It is therefore critical to reach an understanding of how complexation affects the structure-dynamics relationship of the guest (LA) compounds. Investigation of the complexes requires an ensemble of techniques and concepts. For example, because of the expected changes in the thermal properties, such as the loss of endothermic melting peak of the crystalline drug as well as changes in the cyclodextrin cage hydration (Moraes et al., 2006; Specogna et al., 2015), thermal analysis, including differential scanning calorimetry (DSC) and thermogravimetric analysis (TGA), is considered one of most useful approaches for the determination of a successful complexation process. Infrared spectroscopy (IR) and Raman scattering (RS) normally supplement such an analysis. Relevant spectroscopic changes may, however, be difficult to observe (Pinto et al., 2004) since the mass of LA molecules does not exceed 5–15% of the mass of the entire complex. In addition, due to the lack of long-range order, the intermolecular vibrations (lattice modes) are not observed in the complex (Junco et al., 2002; Partanen et al., 2002), and consequently the far-IR region cannot provide useful results. Nuclear magnetic resonance (NMR) spectroscopy has frequently been used for studies of the formation of cyclodextrin complexes (Partanen et al., 2002). For BVC and RVC it has been shown by NMR, for example, that after complexation the aromatic ring of the LA's penetrates into the CD cavity while the butyl chain (methyl 3) remains outside the cage and interacts with external protons of the sugar near the cavity (De Paula et al., 2010; Pinto et al., 2004). However, characterization of LA:CD complexes by means of NMR can be affected by poor solubility of the samples in deuterated ($^2$H NMR) or in pure water ($^{13}$C NMR), so that the use of solvents, which may alter the physical-chemical properties of the complexes, may be required (Lai et al., 2003). Moreover, the lack of symmetry of some of the β-CD derivatives may result in NMR spectra that are not well-resolved (Mura, 2014). In view of the limitations of the techniques described above for reaching an understanding of the dynamics of the complexed LAs, we take an approach that to date has not been fully exploited; namely a combination of standard thermodynamic analysis with incoherent inelastic neutron scattering (IINS) studies and computational investigation by means of density functional theory (DFT). Spectroscopy using IINS is regarded as a relatively unique approach to complement NMR studies since neutrons penetrate matter easily, are sensitive to hydrogen and can access molecular motions occurring on different timescales. Furthermore, special sample preparation is not required for IINS experiments and both external and internal vibrational modes can be observed in a single measurement. Combining IINS experimental spectra with theoretical analysis by means of DFT, then makes it possible to characterize the vibrational modes and to determine which molecular groups contribute most to each part of the IINS spectra (Martins et al., 2016).

Here we demonstrate that this methodology shows that complexation of BVC and RVC in HP-β-CD, hereafter HP-β-CD-BVC and HP-β-CD-RVC, respectively, hinders the motions of the aromatic and piperidine rings as well as the flexibility of the

methyl groups. In addition, our results infer that the effects of complexation on the mobility of BVC are more severe than those on RVC.

## 2. Materials and methods

### 2.1. Materials

BVC hydrochloride monohydrate in the form of racemate (BVC.HCl, $C_{18}H_{28}N_2O{\cdot}HCl{\cdot}H_2O$) and S-RVC hydrochloride monohydrate (RVC.HCl, $C_{17}H_{26}N_2O{\cdot}HCl{\cdot}H_2O$) were donated by Cristália Prod. Quím. Farm. Ltda (Itapira, SP, Brazil). HP-β-CD (Kleptose HP®) was obtained from Roquette Serv. Tech. Lab. (Lestrem, France) and the HEPES buffer was purchased from Sigma Chem. Comp. (St. Louis, MO, USA). Deionized water (Elga Maxima System, Elga, High Wycombe, UK) was used throughout the experiments. All other reagents were of analytical grade.

### 2.2. Sample preparation

Inclusion complexes were prepared by stirring equimolar amounts of the LAs (racemate BVC.HCl and S-RVC.HCl) and HP-β-CD (1:1 molar ratio) in deionized water at room temperature (25 ± 1 °C) for 24 h. After 4 h complete dissolution and equilibrium were reached and the solution was freeze-dried (Labconco-freeze dry system/Freezone® 4.5) and stored at −20 °C until further use, see Ref. (De Araujo et al., 2008) for details.

### 2.3. Calorimetric analysis

Thermogravimetric analyses were conducted in the pure drugs, HP-β-CD and in both complexes placed in an aluminum oxide crucible into the TGA equipment PERSEUS TG 209 F1 Libra (Netzsch, Germany) coupled with a Fourier Transform Infrared Spectrometer (BRUKER Optics Inc., Germany). To stabilize the initial environment, the sample was kept under an isotherm at 35 °C for 5 min. Afterwards the sample was heated from 35 °C to 350 °C (308–623 K) with a heating rate of 10 °C/min under $N_2$ atmosphere. Temperature and heat flows analysis associated with thermal transitions were also performed for each sample, which were mounted in a pierced aluminum pan, sealed and then placed in the DSC device DSC 214 Polyma (Netzsch, Germany). The measurement cycle started with a 5 min isotherm at 35 °C and the sample was heated at a rate of 10 °C/min under $N_2$ atmosphere up to 300 °C for the cases of BVC, RVC and HP-β-CD-RVC. In turn, to avoid contamination of the instrument, HP-β-CD-BVC and HP-β-CD were heated up to 280 °C.

### 2.4. Neutron scattering experiments and brief background

Information on the methyl group rotations in BVC, RVC, HP-β-CD-BVC and HP-β-CD-RVC, which occur in the ps timescale (Fischer et al., 2013), as well as on the interactions between the pure drug molecules and HP-β-CD were obtained by performing IINS measurements using the time-of-flight (ToF) spectrometer IN6, $\lambda_i$ = 5.1 Å, ΔE = 75 μeV (FWHM), located at the Institute Laue Langevin (ILL, Grenoble, France) at temperatures from 50 to 375 K. Elastic fixed window (EFW) scans on all samples were collected using the backscattering instrument IN13, $\lambda_i$ = 2.23 Å, ΔE = 10 μeV (FWHM) also at the ILL between 20 and 300 K. These data yield the mean square displacements of the hydrogen atoms in all the samples, obtained by means of the Gaussian approximation (Gabel, 2005). Detectors with intensity from Bragg reflections, characteristic of crystalline samples, were eliminated using the program LAMP available at the ILL (Richard et al., 1996) so that mostly the incoherent contributions in the spectra could be analyzed.

The observed quantity in IINS experiments, the scattering function $S(Q,\omega)$, where $Q$ is the modulus of the scattering wave vector and ω is the energy exchange between the sample and the neutrons, contains different molecular contributions and distinguishes different types of motion depending on the temperature and energy resolution (time) range of the spectrometer. We note that the behavior of $S(Q,\omega)$ mainly reflects the motions of hydrogen atoms, as they possess a much larger incoherent scattering cross section than that of any other atom in these systems.

The dynamic structure factor $S(Q,\omega)$ can be decomposed as follows (Bée, 1988):

(i) The elastic signal, $S_E(Q,\omega=0)$, probes scattered neutrons that do not exchange energy with the sample within the energy resolution of the instrument. Within the elastic fixed window (EFW) approach, a decrease in $S_E(Q,\omega=0)$ with temperature can provide insight on how confinement modifies the overall dynamics of the drug molecule when compared with the crystalline material. At low temperatures and on a log-scale, the decrease is linear and corresponds to the Debye-Waller factor (Willis and Pryor, 1975):

$$S(Q,\omega\approx 0)\propto e^{\left(-\frac{<u(T)^2>Q^2}{6}\right)} \quad (1)$$

where $<u(T)^2>$ is the mean square displacement of the hydrogen atoms about their equilibrium positions, which can be extracted from the evolution of the elastic intensity in the following manner:

$$-ln\left[\frac{S(Q,T,\omega\approx 0)}{S(Q,T=20,\omega\approx 0)}\right]=\frac{<u(T)^2>}{6}Q^2 \quad (2)$$

The term $\frac{<u(T)^2>}{6}$ is determined by fitting, with a straight line $ln\left[\frac{S(Q,T,\omega=0)}{S(Q,T=20,\omega=0)}\right]$ as a function of $Q^2$. A suitable $Q^2$ range is chosen by obeying the condition $Q^2<u(T)^2>\leq 2$. This is the so-called Gaussian approximation (Gabel, 2005).

(ii) The quasielastic (QENS) signal, $S_{QENS}(Q,\omega\approx 0)$, describes different types of relaxation processes and diffusive motions that can be thermally activated in the samples. The QENS signal generally consists of a superposition of Lorentzians, each originating from a different motion. The QENS broadening, Γ, is usually related to thermally activated stochastic processes and follows an Arrhenius relation, such that its evolution as a function of temperature can be analysed as:

$$\Gamma(T)=\Gamma_0 e^{-\frac{E_{act}}{k_B T}} \quad (3)$$

where, $\Gamma_0$ is the attempt frequency and $E_{act}$ is related to the activation energy of the particular process such as reorientational motions in the system. The latter model is based on the assumption that the molecule oscillates about its equilibrium orientation for an average time "t" and then reorients.

(iii) The inelastic scattering, $S_{IN}(Q,\omega>0)$, gives information on the external (intermolecular) as well as internal (intramolecular) molecular vibrations in the system. This type of information is complementary to what can be obtained by IR and RS spectroscopies. The measured $S_{IN}(Q,\omega>0)$ can be transformed into the so-called generalized density of states (GDOS) as a function of temperature within the incoherent one-phonon approximation using the software LAMP (Richard et al., 1996) to derive details of the molecular vibrational modes (Squires, 2012; Rols et al., 2007)

$$GDOS=G\left(\left\langle Q\right\rangle,\omega\right)=\frac{1}{N_d}\sum_i S(Q_i,\omega)\times\frac{B(\omega,T)}{Q^2\left(\left\langle\theta\right\rangle,\omega\right)} \quad (4)$$

$G\left(\left\langle Q\right\rangle,\omega\right)$ is obtained by averaging over the scattering angles considered in the experiment with $i$ ranging from the first to the

last detector considered in the summation, $\langle\theta\rangle$ being this averaged scattering angle. $N_d$ is the total number of detectors, and $Q^2\left(\langle\theta\rangle,\omega\right)$ is the scattering vector, which is calculated at each energy transfer for the averaged scattering angle. $B(\omega,T)$ is a function accounting for the population of the modes with temperature. This approximation allows for improving the counting statistics, but implies that weak coherence effects in the scattering are also averaged.

### 2.5. Density functional theory (DFT) calculations

Periodic DFT calculations on the structures and harmonic vibrational frequencies of crystalline BVC and RVC were performed with the VASP (Kresse and Furthmüller, 1996) package using the PBE functional by Perdew, Burke and Ernzerhof (PBE) (Perdew et al., 1996, 1997) along with Vanderbilt ultrasoft pseudopotentials (Vanderbilt, 1990) with a plane wave kinetic energy cut-off of 450 eV as well as a $4\times4\times4$ Monkhorst-Pack (Monkhorst and Pack, 1976) mesh of k-points for sampling the Brillouin zone. This methodology was first applied to optimize the positions of the atoms within the unit cell starting with those from the published crystal structures. The optimized atomic positions in turn were then used to calculate the harmonic frequencies and atomic vibrational amplitudes in crystalline BVC and RVC, for use in calculating the INS spectra including folding with the experimental resolution function using the program aClimax (Ramirez-Cuesta, 2004).

## 3. Results

### 3.1. Thermal analysis: evaluation of the crystalline structure of the samples

Thermogravimetric (TGA) and heat flow (DSC) analysis for all samples are shown in Fig. 2. The TGA and dTGA, defined as the differential of the TGA curve, show a gradual mass loss between 35 °C and 200 °C (see inset of Fig. 2(a) and (b)), most likely related to evaporation of water. The maximum mass loss of 6% in this temperature range is observed for RVC, followed by the racemic BVC with a 2% loss. Significantly higher mass losses are observed above 200 °C, which are related to decomposition of the samples. In addition, it is clear that the decomposition of the pure and complexed drugs, with a maximum decomposition rate given by the minimum of the dTGA curves during the decomposition process, takes place at different temperatures, defined as $T_d$, as follows: $T_d$(HP-β-CD-BVC) = 280 °C < $T_d$(HP-β-CD-RVC) = 285 °C < $T_d$(BVC and RVC) ∼ 320 °C < $T_d$(HP-β-CD) = 330 °C.

Concerning the DSC results, Fig. 2(c) and (d), for racemic BVC and RVC, broad endothermic peaks related to the release of water molecules during a dehydration process (Jug et al., 2010) are observed between 100 °C and 150 °C. The total enthalpy (ΔH) of the dehydration was determined as 0.23 kcal/mol for BVC and 0.71 kcal/mol for RVC. On further heating, BVC presents two exothermic phase transitions at 187 °C and 205 °C (inset of Fig. 2(b)), which are related to recrystallization showing similar enthalpy, ΔH ∼ −0.32 kcal/mol, indicating the transformation from a metastable anhydrous form to another (Sykuła-Zaja et al., 2011;

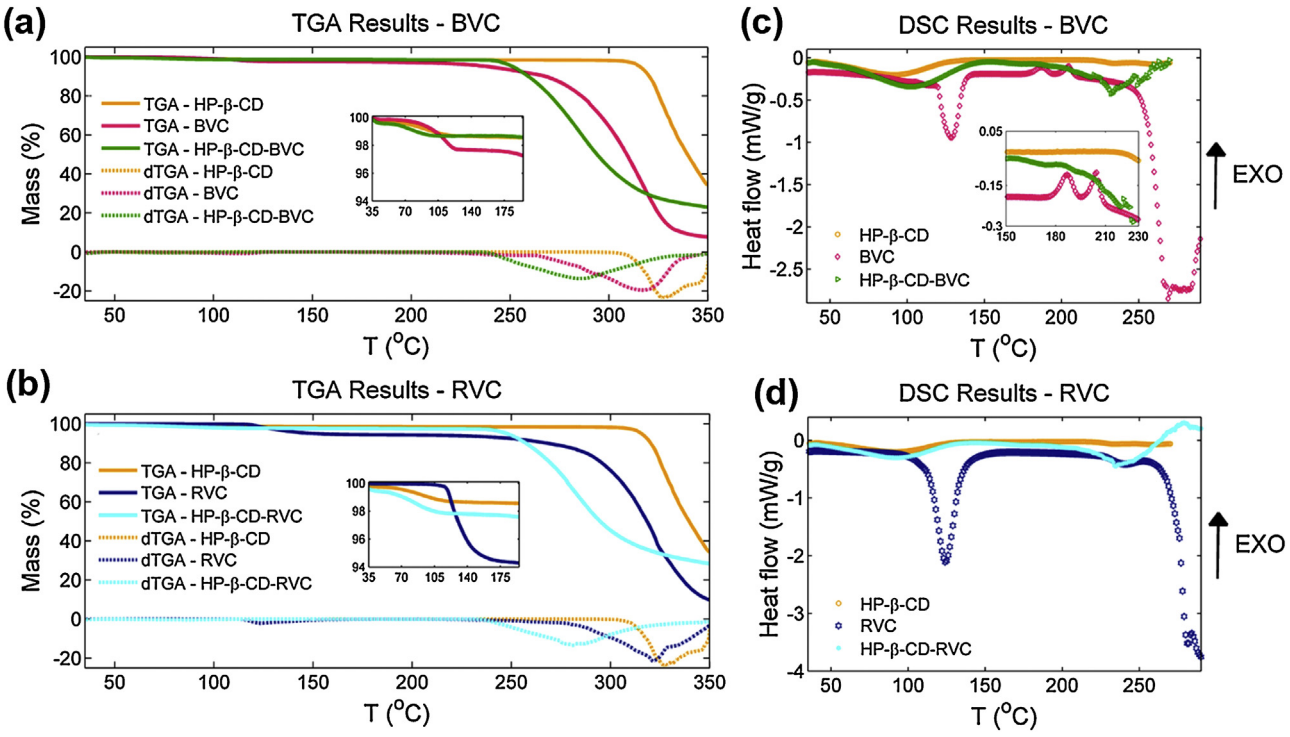


**Fig. 2.** (a) TGA and its derivative (dTGA) of racemic BVC (pink continuous/dashed lines), the complex HP-β-CD-BVC (green continuous/dashed lines) and HP-β-CD (orange continuous/dashed lines). (b) Mass loss of RVC (blue continuous/dashed lines), HP-β-CD-RVC (cyan continuous/dashed lines). For clarity the HP-β-CD data (orange continuous/dashed lines) is reproduced. In (a) and (b) the inset shows in detail the TGA curves from 35 °C to 195 °C. (c) DSC curves obtained using an open crucible of racemic BVC (pink diamonds), the complex HP-β-CD-BVC (green triangles) and HP-β-CD (orange circles), with the inset highlighting the recrystallization processes at 187 °C and 205 °C. Finally, in (d) it is shown the DSC result of RVC (blue stars), HP-β-CD-RVC (cyan asterisks). Here for better comparison the HP-β-CD data (orange circles) is also replicated. All data were obtained using a heating rate of 10 °C/min. To enable the viewing of the decomposition peaks all dTGA curves are multiplied by a factor 10. (For interpretation of the references to colour in this figure legend, the reader is referred to the web version of this article.)

Niederwanger et al., 2008). Finally, the melting process starts around 250 °C for racemic BVC and 260 °C for RVC.

In the case of HP-β-CD, as the water molecules are either in the surface or in the cage, their release is characterized by a broader endothermic peak ranging between 40 °C and 130 °C (De Araujo et al., 2008; Jug et al., 2010; Giordano et al., 2001). This broad transition is preserved in both HP-β-CD-BVC and HP-β-CD-RVC, with slightly wider peak for HP-β-CD-BVC (Fig. 2(b)). The latter observation can be interpreted considering that during complexation the relative humidity inside the cage changes, and a fraction of the water hydrating both pure BVC and RVC creates a different water population inside the cage (Specogna et al., 2015). In addition, differently from the pure compounds, no further transitions are observed between 130 °C and 210 °C in the complexes. The loss of these sharp peaks is a clear sign of amorphization or complexation of the pure drug molecules (Thiry et al., 2017). Finally, the broad endothermic peak with minimum around 235 °C is a further indication of the complexes formation (Thiry et al., 2017). Together, the differences in the decomposition temperatures and in the calorimetric curves are clear manifestations of the reduced thermodynamic activity of the drugs (Pinto et al., 2005; Rengarajan et al., 2008; Wu et al., 2014).

### 3.2. Insights into the dynamical stability using IINS spectroscopy

The effects of complexation on BVC and RVC were investigated by analysis of the QENS spectra collected using the IN6 spectrometer. Due to low counting statistics, a consequence of the removal of the Bragg peaks from the data, all attempts to perform an analysis of the Q-dependence of the motion failed. Thus

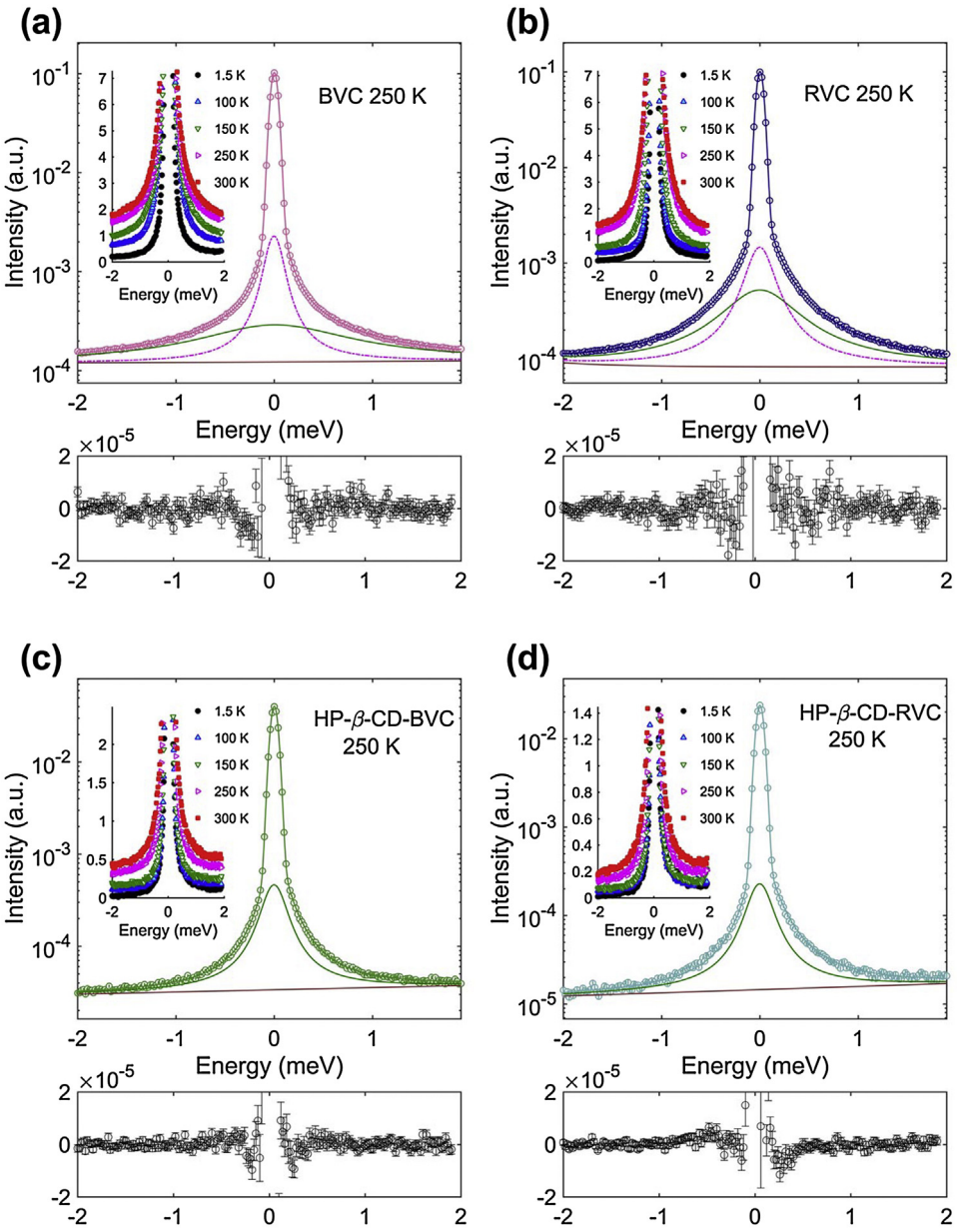


**Fig. 3.** QENS spectra for BVC, RVC, HP-β-CD-BVC and HP-β-CD-RVC obtained using IN6 with a resolution of 75 μeV at 250 K summed over the total Q-range (a–d). The insets show the data collected between 1.5 and 300 K. The dashed lines represent a Dirac function convoluted with the instrument resolution and the full and dotted lines represent Lorentzian functions that describe the thermal activated motions. The full lines in the colors of the respective symbols present the global fits. For all samples the insets were rescaled so the y-axes represents 0.55% of the signal at zero energy transfer at the lowest temperature. Note that the data have not been offset, thus indicating that the increased broadening of the quasielastic signal on heating is entirely due to thermal activation processes. The differences between model and data are also shown. The discrepancies in the model at E = 0 are due to deviations on the Gaussian resolution, thus not impact the fits.

QENS broadening was qualitatively described by fitting the QENS signal summed over Q. The data for both LAs at 250 K are shown in Fig. 3(a) and (b), while the respective insets show the evolution of these QENS spectra with temperature. For BVC, the QENS data at 50, 100 and 150 K can be described by a single Lorentzian within the experimental resolution of the spectrometer, while the data collected above 150 K can only be adequately modeled using an additional Lorentzian function.

The activation energies for the motions described by the first and second Lorentzians ($Ea_{BVC-1}$ and $Ea_{BVC-2}$), Fig. 4(a), were determined from the Arrhenius relation (Eq. (3)) to be 0.36 and 1 kcal/mol (15.6 and 42.5 meV), respectively. For RVC, on the other hand, a single Lorentzian can fit well the experimental data collected below 250 K and results in an activation energy $Ea_{RVC}$ = 0.9 kcal/mol (40.4 meV), Fig. 4(b). No QENS signal was observed within the instrumental resolution for RVC below 100 K. The QENS spectra for the complexed molecules HP-β-CD-BVC and HP-β-CD-RVC (Fig. 3(c) and (d)) are well described in the range between 150 and 300 K by a single Lorentzian with very similar activation energies of ~0.60 kcal/mol (26 meV) for both samples, Fig. 4(a) and (b).

One may attempt to relate the above activation energies to the dynamics of methyl groups by a rather simple approximation if one assumes that the observed QENS broadening from the molecules in the crystal is entirely related to the reorientation of methyl groups in a potential with purely three-fold symmetry. From this assumption one can estimate potential barriers, $V_3$, as well as the energies of the first librational state, $E_{0-1}$, from the activation energy derived above using simplified numerical relations (Bordallo et al., 2010): $E_{0-1}$ (meV) = $0.47[V_3(K)]^{0.548}$ and $E_{act}(K) = 0.598[V_3(K)]^{1.05}$ with the result that one might expect to observe librational modes for the molecules about 9 and 15 meV for BVC (from $Ea_{BVC-1}$ and $Ea_{BVC-2}$, respectively) and approximately 15 meV for RVC (from $Ea_{RVC}$).The temperature evolution of the GDOS for BVC and RVC (Fig. 5(a) and (b)), calculated from the experimental data using Eq. (4) do indeed show very broad bands in these regions, which do, however, contain numerous other vibrational modes. We note that the rotational potential for the methyl groups is unlikely to be of simple three-fold nature on the basis of structural considerations, so that the simple model described above may only be a rough approximation.

It is, of course, not possible to a priori attribute these librational states to a specific methyl group of the molecule, which can only be attempted with the help of the theoretical results from the DFT calculations, which are presented in Fig. 5(c) and (d) for BVC and RVC, respectively. These INS spectra are computed for neutron energy loss at low temperature, while the equivalent experimental data (Fig. 5(a) and (b)) were collected in neutron energy gain at elevated temperatures. This fact accounts for some of the differences between the calculated and observed spectra, along with the anharmonicities in the methyl group librations, which shift these to lower frequencies than those calculated by harmonic DFT.

Each of the calculated vibrational modes can be animated, i.e. visually inspected, using Jmol (The Jmol Team, 2007) in an effort to identify the methyl librational modes, as well as their involvement in other modes. In the case of BVC, relatively pure methyl librations can be found at 17 meV for methyl #2, and 19.8 meV for methyl #1, while the libration for methyl #3 occurs at much higher frequency (26.5 meV) and is more extensively coupled. Methyl librations for RVC are found at 15 meV (#1), and at 31 meV (#3). The torsion for methyl #2 in the case of RVC appears to be coupled to many other modes, so that its frequency therefore could not be precisely determined. Differences in the librational frequencies of chemically identical methyl groups in the two systems can be expected on the basis of crystal packing forces within the two dissimilar structures.

While the effect of the anharmonic potential experienced by the methyl groups on the torsional frequencies cannot be estimated in the absence of an accurate knowledge of the rotational potential, one may be able to use the observed INS intensities and their temperature dependence for assignment of the methyl librations. The very broad band at approximately 20 meV in RVC, for example, may well contain librations from methyl groups #2 and #1, while that for methyl #3 may possibly be assigned to the strong band near 33 meV. The methyl librations in BVC, on the other hand, could conceivably be assigned to the strongly temperature dependent bands at approximately 12 meV (#2), 17 meV (#1) and 25 meV (#3). We may thereby rationalize the observation of just two activation energies (at the resolution provided by IN6) for BVC (from methyls #1 and 2) while in RVC the latter are similar, and possibly coupled, so that only one activation energy is observed. We note that the torsion for methyl #3 would then be subject to a much higher barrier, so that it may not be observable on IN6.

The DFT calculations also serve to understand the behavior of HP-β-CD-BVC and HP-β-CD-RVC, whose experimental GDOS at room temperature are presented in Fig. 6(a) and (b), respectively, together with the spectra obtained for HP-β-CD and that from the corresponding crystalline solid.

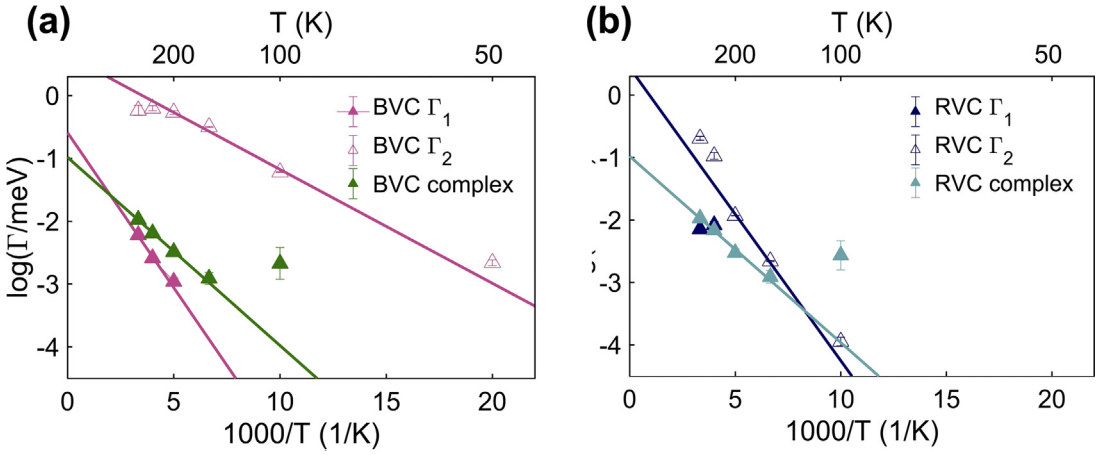


**Fig. 4.** Arrhenius representation of the quasielastic width obtained from the fits of (a) BVC and HP-β-CD-BVC and (b) RVC and HP-β-CD-RVC. The parameter Γ corresponds to the half width half maximum of the Lorentzian functions. The figures only show the data within IN6 resolution range, indicating that below 50 K existing motions in the range of a few picoseconds can no longer be detected.

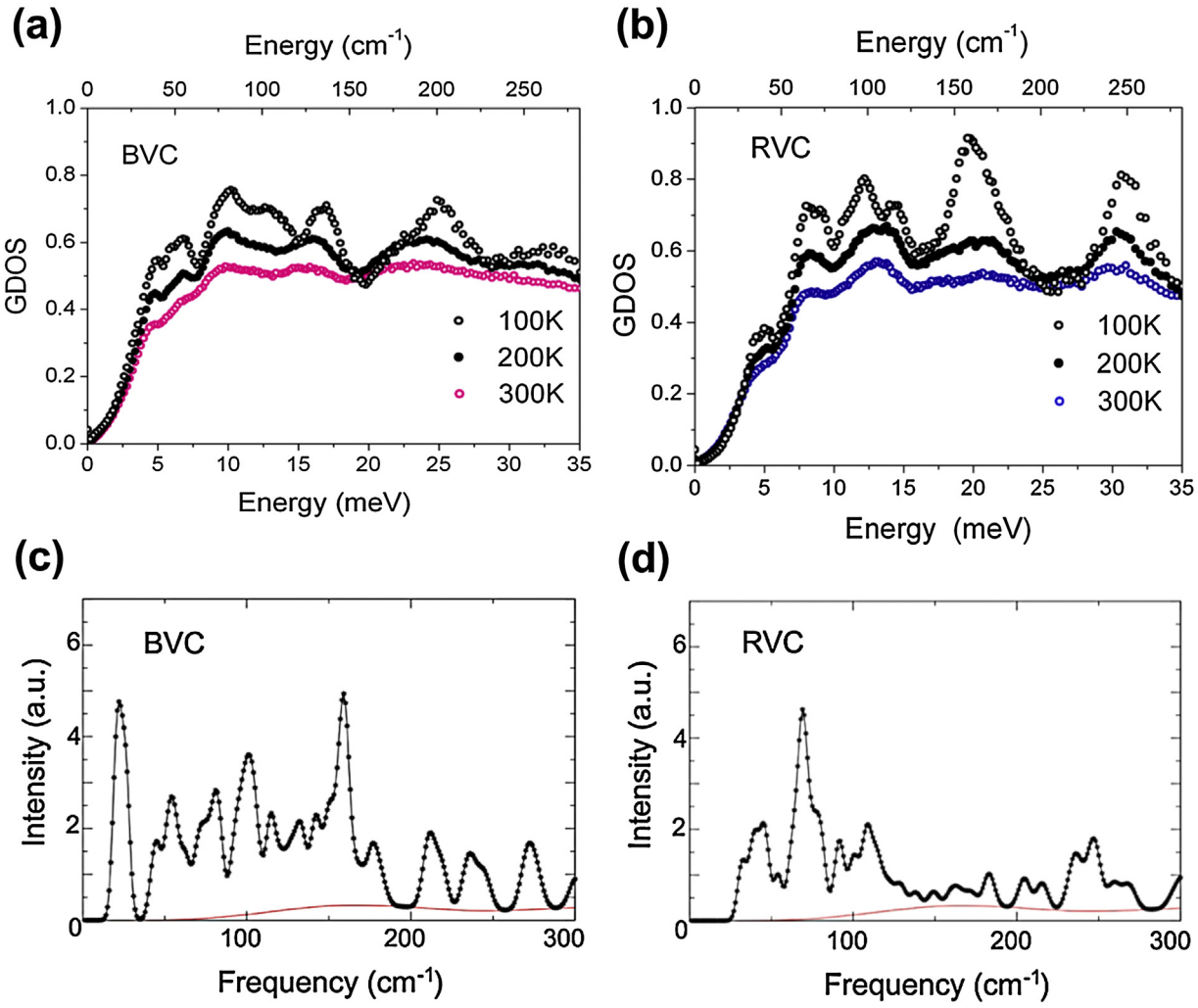


**Fig. 5.** Experimentally determined density of states, (GDOS) of BVC (a) and RVC (b) as a function of temperature obtained using the ToF spectrometer IN6 at the ILL (Grenoble, France). For comparison, the respective spectra theoretically obtained by DFT calculations are shown in (c) and (d). The read lines indicate the multi-phonon contribution.

The existence of broad vibrational modes between 15 and 30 meV in the complexed drug HP-β-CD-BVC suggests that the mobility of all the methyl groups is to a certain extent preserved, as these groups play an important role at this spectral region according to our DFT calculations. These results are in agreement with previous NMR studies for BVC complexed into β-CD (i.e cyclodextrin not modified by the hydroxypropyl groups) (Fraceto et al., 2007).

Moreover, a narrowing, followed by a redshift of the broad vibrational mode located around 55 meV in HP-β-CD-BVC is an indication that the vibrational motions from the H-atoms at the piperidine ring are somewhat restricted after complexation. Such an observation reveals that either the piperidine ring also penetrates into the CD cavity, or it is subject to interactions with external protons of the sugar cage near to the cavity. Finally, as the inclusion of BVC in the sugar cage leads to dehydration of HP-β-CD a consequent smearing out of the librational modes of the water molecules around 75 meV may be noted.

There is also a strong indication in HP-β-CD-RVC that the motions from the piperidine ring are restrained after complexation, as for HP-β-CD-BVC. Some vibrational modes below 35 meV, however, remain apparent in the spectrum of the complexed molecule, and in fact, are better defined than those in HP-β-CD-BVC. We note that the methyl groups contribute significantly in this spectral region. The weaker damping of these modes suggests that the interaction between RVC molecules and the sugar cages is weaker than in the case of BVC. This difference could be important in accounting for the slightly higher stability of HP-β-CD-BVC, as determined using the affinity constant approach (De Araujo et al., 2008; Jug et al., 2010).

This interpretation finds additional support in the analysis of the temperature evolution of $< u(T)^2 >$, which we obtained from the data collected on the IN13 spectrometer (Fig. 7). In both BVC and RVC (Fig. 7(a)) molecular motions are observed at very low temperatures, while at 100 K new motions become fast enough to be observable by the IN13 window as shown by the changes in slope of the respective curves. In BVC the additional slope change is ascribed to a second relaxation process that reaches the instrument time window at 220 K, in agreement with the QENS analysis (i.e. the observation of an additional QENS signal related to $Ea_{BVC-2}$), which leads to higher values of $< u(T)^2 >$, highlighting the greater flexibility of BVC compared with that in RVC. The reduced $< u(T)^2 >$ value for HP-β-CD, also presented in Fig. 7(a), in turn reflects the rigidity of the sugar cage in comparison with the drug molecules. The change of slope around 140 K for these compounds then is most likely related to the activation of OH-motions in HP-β-CD (Jacobsen et al., 2013).

As shown in Fig. 7(b), it is not possible within experimental error of these data to conclusively show if the anesthetics after

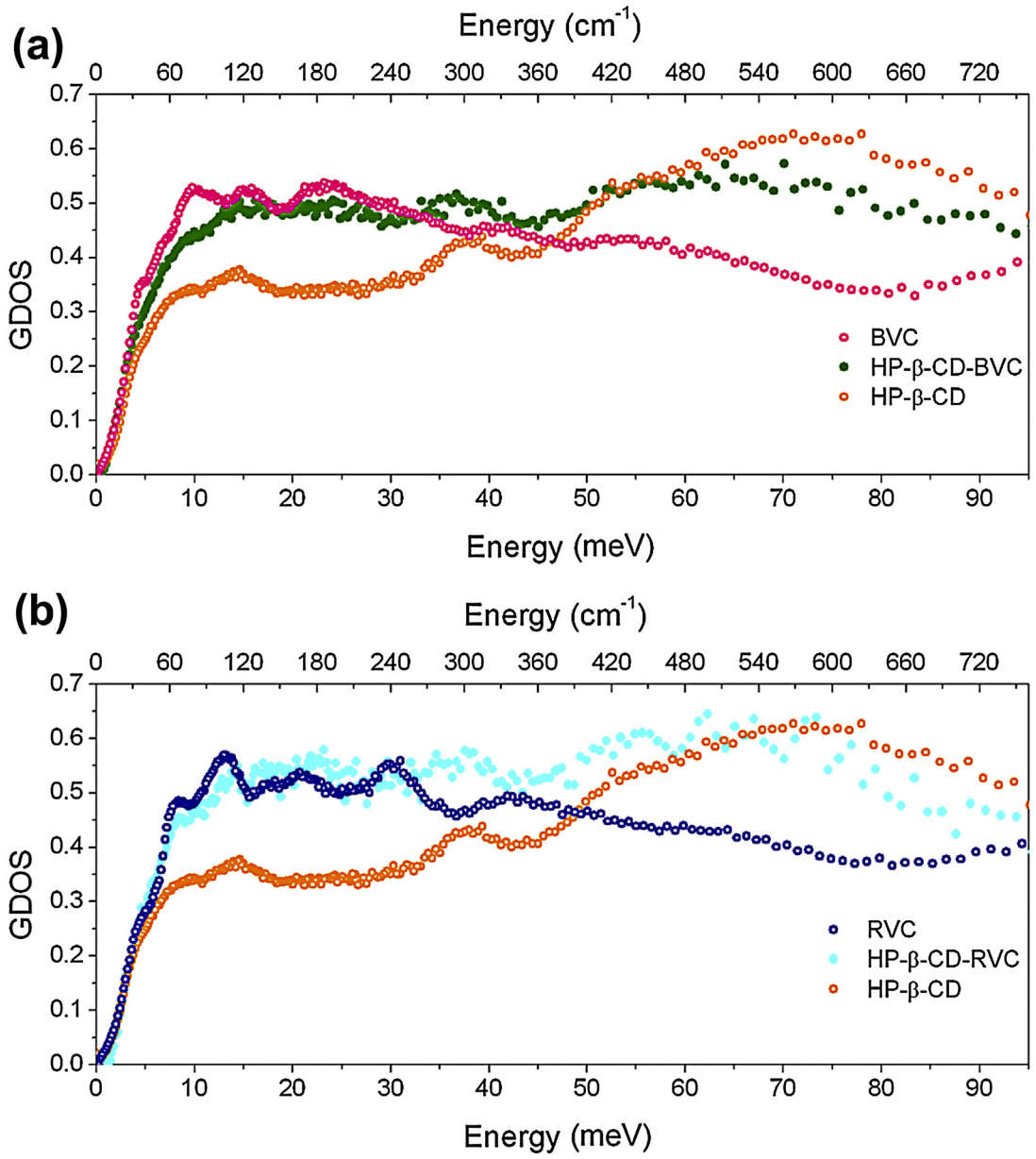


**Fig. 6.** Experimentally determined density of states (GDOS) at room temperature of BVC and HP-β-CD-BVC (a) and RVC and HP-β-CD-RVC (b). The spectrum for HP-β-CD is also presented in (a) and (b).

complexation show different behavior and if the activation of molecular modes occurs at different temperatures. The apparent similarity, however, in the behavior of HP-β-CD-BVC and HP-β-CD-RVC, which was also observed in the QENS analysis described above, confirms that the effects of complexation are indeed more severe for BVC than RVC.

## 4. Conclusions

A combined analysis of incoherent inelastic neutron scattering (IINS) data and theoretical density functional theory (DFT) calculations, leads to a better understanding of the mobility of the local anesthetics molecules bupivacaine (BVC) and ropivacaine (RVC) when complexed by the oligosaccharide HP-β-CD. BVC exhibits a more flexible behavior than RVC because of its racemic character and the presence of an additional C-atom. Despite the differences in dynamics between the crystalline forms of BVC and RVC, their molecular motions on the ps timescale present similar activation energies after complexation. The reason for this is likely to be related to the restriction of the mobility of the aromatic and piperidine rings, as well as a slightly greater hindrance of the reorientation of the methyl groups. The apparent stronger interaction between BVC and HP-β-CD, as compared to the interactions between RVC and the sugar cage, can be related to the higher affinity constant found for HP-β-CD-BVC. Further elucidation of this particular issue, and, consequently, being able to predict the release profiles of complexed drugs is undoubtedly one of the great challenges faced by pharmaceutical technology. Such an understanding would bring to light the possibility of tailoring the drug release rate in accordance with the desired effect. In conclusion, we show that combining DFT with IINS spectroscopic methods is an encouraging approach to overcome this challenge.

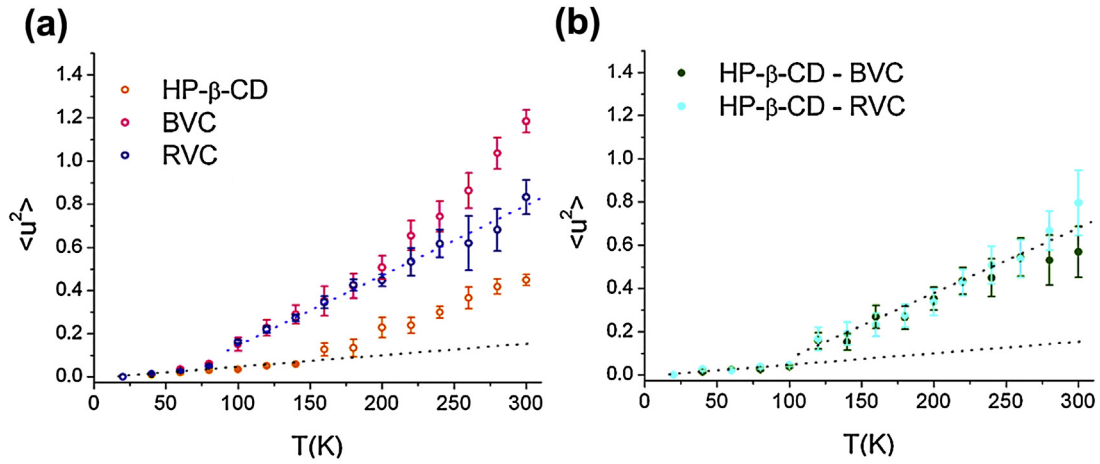


**Fig. 7.** Temperature dependence of $< u(T)^2 >$ for BVC, RVC and HP-β-CD (a) and for HP-β-CD-BVC and HP-β-CD-RVC (b). The dotted lines show the slopes of the curves and depict the flexibility of the investigated molecules. The values were obtained from elastic fixed window (EFW) scans collected in the backscattering instrument IN13 (ΔE = 10 μeV) located at the ILL (Grenoble, France) and are normalized to T = 20 K.

## Author contributions

EP and HNB conceived the project. DRA prepared the samples and RI performed the thermal analysis (TA) together with ECS. AM provided support for the infrared and Raman scattering experiments (showed in the data in brief), which were performed by RI. RI also performed X-ray diffraction experiments whose data are shown in data in brief. HNB designed the neutron scattering experiments, which were carried out by HNB and MCBF with the support from HJ, FN and MMK. HJ and MLM analysed the neutron scattering data, JE carried out the DFT calculations. MLM, JE, ECS and HNB wrote the paper with input from EP. The manuscript was approved by all coauthors.

## Acknowledgements

Work by MLM was financed by the Science without Borders Program (grant number 205609/2014-7) and HJ partially funded by an internship grant offered by the Institute Laue-von-Langevin (ILL). ECS work was financed by the Norwegian Research Council (RCN) SYNKØYT Program (project number 228551). The work of RI was part of a student project and supported by collaboration between HNB and AM. EP acknowledges FAPESP (# 14/1447-5) grant. We acknowledge the support of the ILL in providing the neutron research facilities used in this work. This was financed by NMI3, CoNext and Danscatt. The thermoanalysis apparatus used in the work were financed by Carlsbergfondets (grants 2013_01_0589 and CF14-0230). This research also used resources of the National Energy Research Scientific Computing Center, a DOE Office of Science User Facility supported by the Office of Science of the U.S. Department of Energy under Contract No. DE-AC02-05CH11231. JE would also like to thank the Physics and Chemistry of Materials Group (T-1) at LANL for making computing resources available. HNB thanks Stéphane Rols (ILL) for fruitful discussions concerning the analysis of the quasi-elastic data. We also thank Niels Vissing Holst for technical support on collection of X-ray diffraction data shown in data in brief.

## References

Albright, G.A., 1979. Cardiac arrest following regional anesthesia with etidocaine or bupivacaine. Anesthesiology 51, 285–287.
Bée, M., 1988. Quasielastic Neutron Scattering, Principles and Applications in Solid State, Chemistry, Biology and Materials Science. CRC Press.
Bordallo, H.N., Boldyreva, E.V., Fischer, J., Koza, M.M., Seydel, T., Minkov, V.S., Drebushchak, V.A., Kyriakopoulos, A., 2010. Observation of subtle dynamic transitions by a combination of neutron scattering, X-ray diffraction and DSC: a case study of the monoclinic l-cysteine. Biophys. Chem. 148, 34–41.
De Araujo, D.R., Tsuneda, S.S., Cereda, C.M., Carvalho, F.D.G.F., Prete, P.S.C., Fernandes, S.A., Yokaichiya, F., Franco, M.K.K.D., Mazzaro, I., Fraceto, L.F., Braga, A.F.A., De Paula, E., 2008. Development and pharmacological evaluation of ropivacaine-2-hydroxypropyl-beta-cyclodextrin inclusion complex. Eur. J. Pharm. Sci. 33, 60–71.
De Paula, E., De Araújo, D.R., Fraceto, L.F., 2010. Nuclear Magnetic Resonance Spectroscopy tools for the physicochemical characterization of cyclodextrins inclusion complexes. In: Hu, J. (Ed.), Cyclodextrins: Chemistry and Physics. Research Signpost/Transworld Research Network, pp. 1–21.
Do Prado, J.N., Pissatto, S., De Morais, E.C., Foppa, T., Murakami, F.S., Silva, M.A.S., 2006. Validação de metodologia analítica por cromatografia líquida de alta eficiência para doseamento de cápsulas de fluoxetina. Acta Farm. Bonaer. 25, 436–440.
Fischer, J., Lima, J.A., Freire, P.T.C., Melo, F.E.A., Havenith, R.W.A., Filho, J.M., Broer, R., Eckert, J., Bordallo, H.N., 2013. Molecular flexibility and structural instabilities in crystalline L-methionine. Biophys. Chem. 180–181, 76–85.
Fraceto, L.F., Moraes, C.M., Gonçalves, M.M., Araújo, D.R., Zanella, L., De Paula, E., Pertinhez, T.A., 2007. Caracterização do complexo de inclusão ropivacaína:beta-ciclodextrina. Quím. Nova 30, 1203–1207.
Gabel, F., 2005. Protein dynamics in solution and powder measured by incoherent elastic neutron scattering: the influence of Q-range and energy resolution. Eur. Biophys. J. 34, 1–12.
Giordano, F., Novak, C., Moyano, J.R., 2001. Thermal analysis of cyclodextrins and their inclusion compounds. Thermochim. Acta 380 (2), 123–151.
Gould, S., Scott, R.C., 2005. 2-Hydroxypropyl-beta-cyclodextrin (HP-β-CD): a toxicology review. Food Chem. Toxicol. 43, 1451–1459.
Harmatz, A., 2009. Local anesthetics: uses and toxicities. Surg. Clin. North Am. 89, 597–598.
Huet, O.E.L., Mazoit, J.X., Oxier, Y.M., 2003. Cardiac arrest after injection of ropivacaine for posterior lumbar plexus blockade. Anesthesiology 99, 1451–1453.
Jacobsen, J., Rodrigues, M.S., Telling, M.T.F., Beraldo, A.L., Santos, S.F., Aldridge, L.P., Bordallo, H.N., 2013. Nano-scale hydrogen-bond network improves the durability of greener cements. Sci. Rep. 3, 2667.
Jug, M., Maestrelli, F., Bragagni, M., Mura, P., 2010. Preparation and solid-state characterization of bupivocaine hydrochloride cyclodextrin complexex aimed for bucal delivery. J. Pharm. Biomed. Anal. 52, 9–18.
Junco, S., Casimiro, T., Ribeiro, N., Da Ponte, M.N., Marques, H.C., 2002. A comparative study of naproxen—beta cyclodextrin complexes prepared by conventional methods and using Supercritical carbon dioxide. J. Incl. Phenom. Macrocyclic 44, 117–121.
Kresse, G., Furthmüller, J., 1996. Efficient iterative schemes for ab initio total-energy calculations using a plane-wave basis set. Phys. Rev. B—Condens. Matter Mater. Phys. 54, 11169–11186.
Lai, S., Locci, E., Piras, A., Porcedda, S., Lai, A., Marongiu, B., 2003. Imazalil-cyclomaltoheptaose (beta-cyclodextrin) inclusion complex: preparation by supercritical carbon dioxide and C-13 CPMAS and H-1 NMR characterization. Carbohydr. Res. 338, 2227–2232.
Loftsson, T., Duchêne, D., 2007. Cyclodextrins and their pharmaceutical applications. Int. J. Pharm. 329, 1–11.
Magalhães, E., Gôveia, C.S., Oliveira, K.B., 2004. Racemic bupivacaine, levobupivacaine and ropivacaine in regional anesthesia for ophtalmology. Rev. Assoc. Med. Bras. 50, 195–198.

Marques, H.M.C., 2010. A review on cyclodextrin encapsulation of essential oils and volatiles. Flavour Fragr. J. 25, 313–326.
Martins, M.L., Ignazzi, R., Eckert, J., Watts, B., Kaneno, R., Zambuzzi, W.F., Daemen, L., Saeki, M.J., Bordallo, H.N., 2016. Restricted mobility of specific functional groups reduces anti-cancer drug activity in healthy cells. Sci. Rep. 6, 22478.
McLure, H.A., Rubin, A.P., 2005. Review of local anaesthetic agents. Minerva Anestesiol. 71, 59–74.
Monkhorst, H., Pack, J., 1976. Special points for Brillouin zone integrations. Phys. Rev. B 13, 5188–5192.
Moraes, C.M., Issa, M.G., Ferraz, H.G., Yokaichiya, F., Franco, M.K.K.D., Mazzaro, I., Lopes, P.S., Gonçalves, M.M., De Paula, E., Fraceto, L.F., 2006. Inclusion complex of S(−) bupivacaine and 2-hydroxypropyl-beta-cyclodextrin: study of morphology and cytotoxicity. Rev. Ciências Famacêuticas Básica Apl. 27, 207–212.
Mura, P., 2014. Analytical techniques for characterization of cyclodextrin complexes in aqueous solution: a review. J. Pharm. Biomed. Anal. 101, 238–250.
Niederwanger, V., Gozzo, F., Griesser, U.J., 2008. Characterization of four crystal polymorphs and a monohydrate of s-bupivacaine hydrochloride (levobupivacaine hydrochloride). J. Pharm. Sci. 98 (3), 1064–1074.
Partanen, R., Ahro, M., Hakala, M., Kallio, H., Forssell, P., 2002. Microencapsulation of caraway extract in (-cyclodextrin and modified starches. Eur. Food Res. Technol. 214, 242–247.
Perdew, J., Burke, K., Ernzerhof, M., 1996. Generalized gradient approximation made simple. Phys. Rev. Lett. 77, 3865–3868.
Perdew, J.P., Burke, K., Ernzerhof, M., 1997. Generalized gradient approximation made simple. Phys. Rev. Lett. 78, 1396 Erratum to document cited in CA126:51093.
Pinto, L.M.A., De Jesus, M.B., De Paula, E., Lino, A.C.S., Alderete, J.B., Duarte, H.A., Takahata, Y., 2004. Elucidation of inclusion compounds between β-cyclodextrin/local anaesthetics structure: a theoretical and experimental study using differential scanning calorimetry and molecular mechanics. J. Mol. Struct. THEOCHEM 678, 63–66.
Pinto, L.M.A., Fraceto, L.F., Santana, M.H.A., Pertinhez, T.A., Junior, S.O., De Paula, E., 2005. Physico-chemical characterization of benzocaine-(-cyclodextrin inclusion complexes. J. Pharm. Biomed. Anal. 39 (5), 956–963.
Rajabi, O., Tayyari, F., Salari, R., Tayyari, S.F., 2008. Study of interaction of spironolactone with hydroxypropyl-beta-cyclodextrin in aqueous solution and in solid state. J. Mol. Struct. 878, 78–83.
Ramirez-Cuesta, A.J., 2004. aCLIMAX 4.0.1, the new version of the software for analyzing and interpreting INS spectra. Comput. Phys. Commun. 157, 226–238.
Rengarajan, G.T., Enke, D., Steinhart, M., Beiner, M., 2008. Stabilization of the amorphous state of pharmaceuticals in nanopores. J. Mater. Chem. 18, 2537–2539.
Richard, D., Ferrand, M., Kearley, G.J., 1996. Analysis and visualisation of neutron-scattering data. J. Neutron Res. 4, 33–39.
Rols, S., Jobic, H., Schober, H., 2007. Monitoring molecular motion in nano-porous solids. C. R. Phys. 8, 777–788.
Ruetsch, Y.A., Böni, T., Borgeat, A., 2001. From cocaine to ropivacaine: the history of local anesthetic drugs. Curr. Top. Med. Chem. 1, 175–182.
Scott, D.B., Lee, A., Fagan, D., Bowler, G.M., Bloomfield, P., Lundh, R., 1989. Acute toxicity of ropivacaine compared with that of bupivacaine. Anesth. Analg. 69, 563–569.
Specogna, E., Li, K.W., Djabourov, M., Carn, F., Bouchemal, K., 2015. Dehydration dissolution, and melting of cyclodextrin crystals. J. Phys. Chem. B 119, 1433–1442.
Squires, G.L., 2012. Introduction to the Theory of Thermal Neutron Scattering, 3rd ed. Cambridge University Press, Cambridge.
Sykuła-Zaja, A., Łodyga-Chruscinska, E., Pałecz, B., Dinnebier, R.E., Griesser, U.J., Niederwanger, V., 2011. Thermal and X-ray analysis of racemic bupivacaine hydrochloride. J. Therm. Anal. Calorim. 105, 1031–1036.
The Jmol Team, 2007. Jmol: An Open-source Java Viewer for Chemical Structures in 3D. http://jmol.sourceforge.net (accessed 30 September 2016).
Thiry, J., Krier, F., Ratwatte, S., Thomassin, J., Jerome, B., Evrard, B., 2017. Hot-melt extrusion as a continuous manufacturing process to form ternary cyclodextrin inclusion complexes. Eur. J. Pharm. Sci. 96, 590–597.
Vanderbilt, D., 1990. Soft self-consistent pseudopotentials in a generalized eigenvalue formalism. Phys. Rev. B 41, 7892–7895.
Willis, B.T.M., Pryor, A.W., 1975. Thermal Vibrations in Crystallography. Cambridge University Press, Cambridge.
Wu, D., Hwang, S., Zones, S.I., Navrotsky, A., 2014. Guest-host interactions of a rigid organic molecule in porous silica frameworks. PNAS 111 (5), 1720–1725.